AGU PUBLICATIONS

Water Resources Research

RESEARCH ARTICLE
10.1002/2017WR020411

Key Points:
- Pedotransfer functions are proposed to estimate WRC from two basic soil gradation parameters (d_{10} and C_u) through a semiempirical approach
- With physical features considered, the model with fewer and more easily obtained parameters shows good performance in WRC prediction
- By incorporating with the suction stress definition, it provides a preliminary estimation of strength properties from grain size

Correspondence to:
J.-P. Wang,
Ji-Peng.Wang@ulb.ac.be;
Ji-Peng.Wang@outlook.com

Citation:
Wang, J.-P., N. Hu, B. François and P. Lambert (2017), Estimating water retention curves and strength properties of unsaturated sandy soils from basic soil gradation parameters, *Water Resour. Res.*, *53*, 6069–6088, doi:10.1002/2017WR020411.

Received 1 FEB 2017
Accepted 26 JUN 2017
Accepted article online 5 JUL 2017
Published online 25 JUL 2017

Estimating water retention curves and strength properties of unsaturated sandy soils from basic soil gradation parameters

Ji-Peng Wang[1], Nian Hu[2], Bertrand François[1], and Pierre Lambert[3]

[1]Building Architecture and Town Planning Department, Université Libre de Bruxelles, Brussels, Belgium, [2]Nottingham Centre for Geomechanics, Faculty of Engineering, University of Nottingham, University Park, Nottingham, UK, [3]BEAMS Department, Université Libre de Bruxelles, Brussels, Belgium

Abstract This study proposed two pedotransfer functions (PTFs) to estimate sandy soil water retention curves. It is based on the van Genuchten's water retention model and from a semiphysical and semistatistical approach. Basic gradation parameters of d_{60} as particle size at 60% passing and the coefficient of uniformity C_u are employed in the PTFs with two idealized conditions, the monosized scenario and the extremely polydisperse condition, satisfied. Water retention tests are carried out on eight granular materials with narrow particle size distributions as supplementary data of the UNSODA database. The air entry value is expressed as inversely proportional to d_{60} and the parameter n, which is related to slope of water retention curve, is a function of C_u. The proposed PTFs, although have fewer parameters, have better fitness than previous PTFs for sandy soils. Furthermore, by incorporating with the suction stress definition, the proposed pedotransfer functions are imbedded in shear strength equations which provide a way to estimate capillary induced tensile strength or cohesion at a certain suction or degree of saturation from basic soil gradation parameters. The estimation shows quantitative agreement with experimental data in literature, and it also explains that the capillary-induced cohesion is generally higher for materials with finer mean particle size or higher polydispersity.

1. Introduction

For unsaturated soils, the water retention curve (WRC) or the soil water characteristic curve (SWCC), which represents the relationship between water content and suction, is a crucial function for determining both the soil hydraulic property and its coupled mechanical properties. It has long been aware that the WRC is correlated to soil properties like the soil particle size distribution (PSD), soil texture (such as percentage of silt, clay, and organic matter), and bulk density (or void ratio) [*Gupta and Larson*, 1979; *Saxton et al*., 1986; *Vereecken et al*., 1989] which may be referred as pedotransfer functions (PTFs) [*Bouma*, 1989]. For a soil with large clay or organic contents, its microstructure or fabric may be more complicated due to its physicochemical interactions. And for a sandy soil, regarding its relatively small void ratio variation, its WRC may be directly predicted from its PSD, which may provide a fast and inexpensive way of WRC estimation.

Strength properties of unsaturated soils are required to be understood for various geotechnical problems such as slope stability, embankment, and pavement design. A number of efforts on studying strength properties of unsaturated soils have been carried out on shear strength criteria [*Fredlund et al*., 1978, 1987; *Vanapalli et al*., 1996; *Oberg and Sällfors*, 1997; *Khalili and Khabbaz*, 1998; *Vanapalli and Fredlund*, 2000; *Tekinsoy et al*., 2004; *Konrad and Lebeau*, 2015; *Zhou et al*., 2016] or on the understanding of tensile strength or cohesion [*Schubert et al*., 1975; *Turner et al*., 1976; *Kim and Hwang*, 2003; *Matsushi and Matsukura*, 2006; *Lu et al*., 2007, 2009]. The strength properties are recognized to be closely related to water content or suction. The degree of saturation (and recently the term of effective degree of saturation) obtained from the WRC at a certain suction value is usually imbedded in equations describing the strength properties [*Fredlund et al*., 1996; *Vanapalli et al*., 1996; *Oberg and Sällfors*, 1997; *Lu et al*., 2007, 2010; *Alonso et al*., 2010; *Konrad and Lebeau*, 2015]. Thus, if the WRC can be estimated from soil gradation, its strength properties at a certain degree of saturation or suction can be preliminarily estimated. This may be helpful for engineering projects at an early stage when not much experimental data are available.

One approach to predict WRC, from a physicoempirical way, is based on assumptions that the particles are spherical and the pores can be simplified as cylindrical shapes. *Arya and Paris* [1981] proposed the first physicoempirical model (AP model) by assuming that a PSD consists of a number of single particle size fractions and each fraction provides a weighted contribution to the pore size distribution and thus the WRC can be estimated from the particle size distribution based on a scaling factor. Following the AP model, different predictions have been developed with further modification by using improved mathematical expressions on PSD [*Fredlund et al*., 2002; *Hwang and Powers*, 2003] and the scaling factor [*Haverkamp and Parlange*, 1986; *Tyler and Wheatcraft*, 1989; *Arya et al*., 1999]. Another approach to estimating WRC from PSD, following the PTF terminology, is a statistical method of formulating the parameters of a closed-form WRC function from soil gradation parameters based on regression analysis. *Saxton et al*. [1986] and *Vereecken et al*. [1989] proposed basic formulations by using soil texture fractions. While in the later models [*Scheinost et al*., 1997; *Schaap and Leij*, 1998], WRC parameters are estimated from a measure of mean particle size and a measure of particle size uniformity. Recently, *Chiu et al*. [2012] improved the expression of PTF by using a Bayesian probabilistic method to choose the best model from a list of possible mathematical expression forms.

The physicoempirical approach considers basic physical properties, but it is based on a list of simple assumptions and cannot avoid empirical coefficients. The required number of measured parameters of a physicoempirical model is usually large, which makes this approach less applicable in geotechnical engineering practice, as sometimes a preliminary estimation is required with some degree of accuracy can be sacrificed. On the other hand, the purely statistical approach, which does not consider much of the physical background, may be not always valid beyond the modeled database. In this study, we try to propose PTFs in a semiphysical and semistatistical way based on simple soil gradation parameters. The widely used *van Genuchten's* model [*van Genuchten*, 1980] is employed to describe the WRC. By using dimensional analysis [*Buckingham*, 1914], the key links between the WRC and the PSD are clarified. Two idealized conditions, a monosized packing and an extremely polydisperse packing, are considered on the basis of the physical features. Regression analysis is then carried out based on the first drying WRCs of 70 soils from the UNSODA database [*Leij et al*., 1996] and 8 granular soils we tested and the PTF is obtained by using parameters of d_{60} and C_u. After validations of the PTFs, by coupling with the suction stress definition [*Lu and Likos*, 2006; *Lu et al*., 2010], the shear strength and capillary cohesion are then formulated and discussed in terms of the basic soil gradation parameters. It should be noted that the proposed estimations of WRC and strength properties are more suitable for sandy soils with continuous PSDs without gaps. This study is based on the first drying path that can be considered as a unique curve for a certain soil. On the contrary, wetting curves depend on the suction maximum in the drying path where the wetting curve starts. Consequently, the hysteresis effect is therefore not considered and needs future works.

2. General Relationship Between WRC, Strength, and PSD

2.1. Van Genuchten's Model for Water Retention Behavior

To dry a soil from a fully saturated condition (see Figure 1a), with the increase of soil suction, the degree of saturation may not be obviously decreased until the air entry value (AEV). Then, air bubbles may be entrapped into the water phase. In this stage, the water phase is a continuous phase and the air phase is discontinuous, sometimes it is also referred to the capillary state. Consequently, moisture content starts to reduce significantly with suction and both water and air phases become continuous (this is also referred to the funicular state) [*Wang et al*., 2017]. At a relatively high suction, water phase becomes discontinuous as isolated water bridges and adsorption layers (the pendular state) and thus an enormous suction is required to dry the residual water out. This state is referred to the residual state. To characterize water retention behaviors in the active range, the residual state is usually not considered and a definition of the effective degree of saturation is adopted as

$$S_e = \frac{\theta - \theta_r}{\theta_s - \theta_r} = \frac{S_r - S_r^r}{1 - S_r^r} \tag{1}$$

where θ, θ_s, and θ_r are water content, saturated water content, and residual water content, respectively, and S_r and S_r^r are the degree of saturation and the residual degree of saturation. In the widely used *van Genuchten's* model [*van Genuchten*, 1980], the water retention curve is expressed as

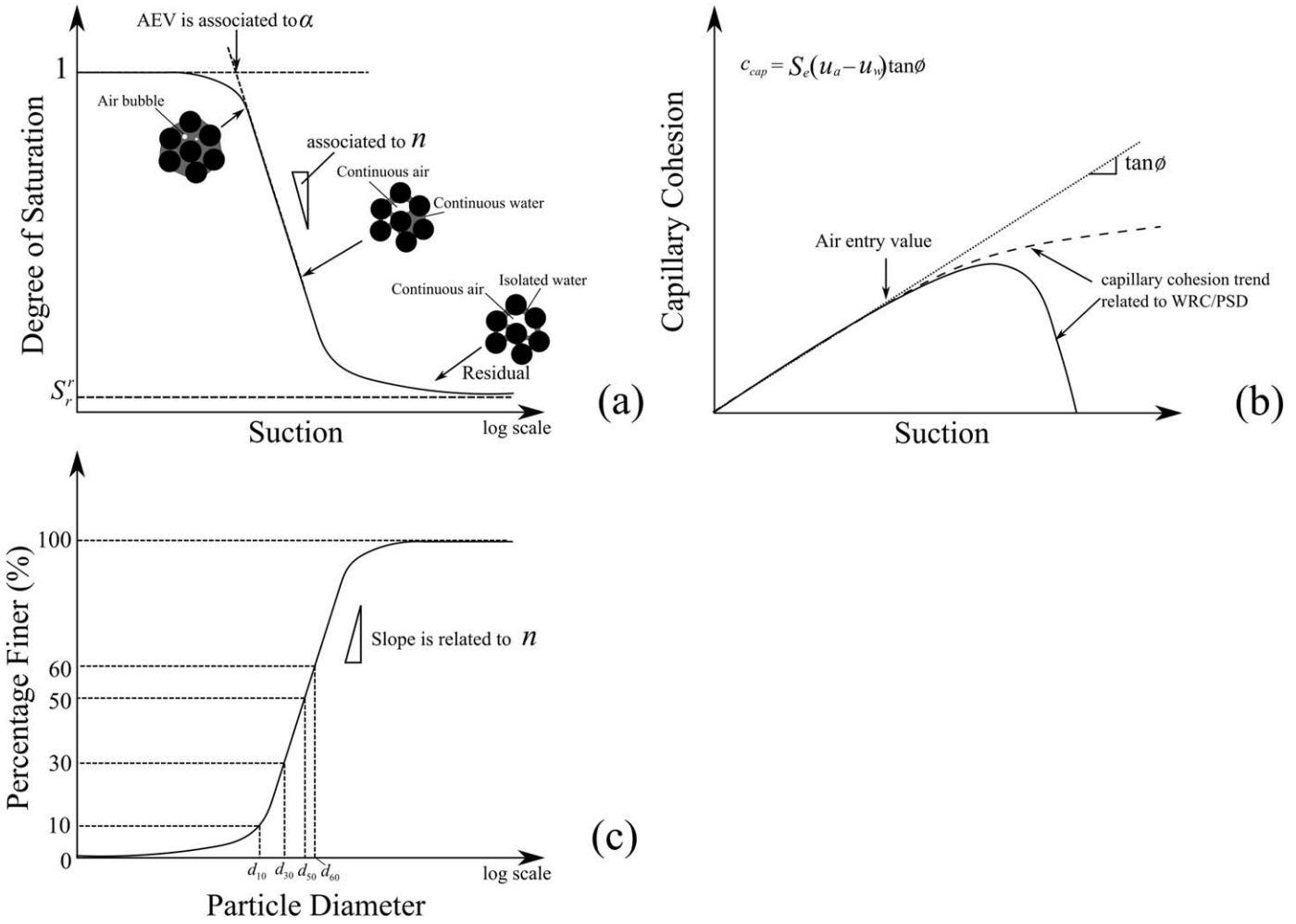

Figure 1. Sketches of (a) water retention curve, (b) capillary cohesion, and (c) particle size distribution.

$$S_e = \left(1 + \left(\frac{\psi}{\alpha}\right)^n\right)^{\frac{1}{n}-1} \tag{2}$$

where ψ is soil suction (equals to the pressure difference between air and water phase, $u_a - u_w$), α is a parameter related to air entry value, and n is a parameter related to the slope of the water retention curve.

2.2. General Relationship Between WRC and Strength

The mechanical behavior of an unsaturated sandy soil is usually investigated based on its "effective stress" which is assumed to be transmitted through the soil skeleton. After *Bishop and Blight* [1963], the effective stress of unsaturated soil is expressed as

$$\sigma' = (\sigma - u_a) + \chi(u_a - u_w) \tag{3}$$

where σ is total stress, u_a is air pressure, u_w is water pressure, and the Bishop's coefficient χ is assumed to be related to the degree of saturation that $\chi = 0$ when the soil is completely dry and $\chi = 1$ when it is fully saturated. The difference between air and water pressure, $u_a - u_w$, is the matrix suction ψ. After a microstructural analysis, *Lu and Likos* [2006] proposed that a "suction stress" definition, which is in coupling with the water retention behavior, can be used to determine the stress state and they express the effective stress as

$$\sigma' = (\sigma - u_a) - \sigma_s \tag{4}$$

where σ_s is the suction stress and when the soil is fully saturated $\sigma_s = 0$. Later, the closed form of suction stress is formulated by *Lu et al.* [2010] by multiplying the effective degree of saturation and the matric suction as $\sigma_s = -S_e(u_a - u_w)$, thus, the effective stress can be expressed as

$$\sigma' = (\sigma - u_a) + S_e(u_a - u_w) \tag{5}$$

where the effective degree of saturation can be formulated by the *van Genuchten's* model in equation (2). The definition of suction stress shows fair validations in different soils from clays to sands [*Lu et al.*, 2010; *Oh et al.*, 2012; *Oh and Lu*, 2014] and using S_e as the χ value can also be seen in *Vanapalli et al.* [1996]. Although it has been argued that corrected exponential expressions like $\chi \approx S_e^{\beta}$ [*Alonso et al.*, 2010] may be more accurate for some soils, by taking $\chi \approx S_e$ provides great convenience for preliminary strength estimation from water retention curve and soil gradation in the following study. The shear strength can then be expressed based on the classical Mohr-Coulomb failure criterion with the suction stress definition incorporated:

$$\tau = (\sigma - u_a)\ \tan\phi + S_e(u_a - u_w)\ \tan\phi + c' \tag{6}$$

where ϕ is the internal friction angle and c' is the effective cohesion. For sandy soils, other cohesive effects like the van der Waals force and the cementation effect are very small, which leads c' to be negligible and leaves the capillary cohesion, noted as $c_{cap} = S_e(u_a - u_w)\tan\phi$, to be the main water induced strength increment. By increasing suction, the capillary cohesion increased with the friction angle until it reaches the air entry value. Then, the slope of capillary cohesion increase is smaller. Depending on the water retention curve, which is related to particle size distribution, further increase in suction (decrease in water content) may result in a modest increase in capillary cohesion or a weakened strength when the material is nearly dried. A conceptual figure can be seen in Figure 1b presenting the relationship between suction and capillary cohesion.

2.3. Summary of PTFs Based on Van Genuchten's Model

The mechanical behaviors have coupling effect with WRC and the WRC can be determined from soil gradation parameters according to the PTF concept. Numerous efforts have been carried out on the development of pedotransfer functions in the past three decades. Recent state of the arts about the PTF development can be seen in *Vereecken et al.* [2010] and *Patil and Singh* [2016]. Basically, the PTFs can be categorized into two types: points PTFs in which water content values are estimated at certain suctions [*de Jong and Loebel*, 1982; *Rawles and Brakensiek*, 1982; *Puckett et al.*, 1985] and parametric PTFs by estimating the parameters of continuous functions describing the WRC [*Wösten and van Genuchten*, 1988; *Vereecken et al.*, 1989; *Schaap et al.*, 2001; *Ghanbarian-alavijeh et al.*, 2010]. Recently, the second type is more common as it can be further employed in other analytical models. The *van Genuchten's* model is the most popular model adopted in this approach.

There is a list of pedotransfer functions based on the *van Genuchten's* model, in which the parameters of α and n are estimated from soil particle size distribution data. A good summary can be seen in *Chiu et al.* [2012]. In the early study, the PTFs are usually developed by using predictors of sand, silt and clay fractions as well as bulk densities [*Vereecken et al.*, 1989]. This type of model covers all kind of soils but usually has lower accuracy for some particular materials. Then, specified to sandy soils, *Schaap and Bouten* [1996] describe the particle size distribution as a continuous function:

$$F(d) = \left(1 + \left(\frac{d_p}{d}\right)^{n_p}\right)^{\frac{1}{n_p}-1} \tag{7}$$

where $F(d)$ is the cumulative fraction of particle size d and d_p and n_p are fitting parameters of the particle size distribution in which d_p reflects the mean particle size and n_p is a measure of particle size uniformity. After a neural network analysis, *Schaap and Bouten* [1996] formulated α to be inversely proportional to d_p and n to be a function of n_p and bulk density. Later, *Scheinost et al.* [1997] and *Minasny et al.* [1999] used geometrical mean particle size (d_g) and standard deviation (σ_g) as the key parameters to characterize particle size distributions as

$$d_g = \exp\left[\sum_{i=1}^{t} f_i \ln(m_i)\right] \tag{8}$$

$$\sigma_g = \exp\left[\sqrt{\sum_{i=1}^{t} f_i \ln^2(m_i) - \left(\sum_{i=1}^{t} f_i \ln(m_i)\right)^2}\right] \tag{9}$$

where m_i is the logarithm mean of the ith fraction, f_i is the amount of the ith fraction, and t is the total number of fractions. *Scheinost et al.* [1997] then interpreted the parameter α as a function of d_g and the

Table 1. Summary of Pedotransfer Functions Based on the *van Genuchten's* Model [After *Chiu et al.*, 2012][a]

	α	n
Vereecken et al. [1989]	$\ln(\alpha)=\alpha_0+\alpha_1 S+\alpha_2 CL+\alpha_3 C+\alpha_4 BD$	$\ln(n)=n_0+n_1 S+n_2 CL+n_3 S^2$
Schaap and Bouten [1996]	$\alpha=\frac{1}{\alpha_0+\alpha_1 d_p}$	$\log(n)=n_0+n_1\log(n_p)+n_2 BD$
Scheinost et al. [1997]	$\alpha=\frac{1}{\alpha_0+\alpha_1 d_g}$	$n=n_0+n_1\sigma_g{}^{-1}$
Chiu et al. [2012]	$\alpha=\frac{1}{\alpha_0+\alpha_1 d_{50}}$	$n=n_0+n_1\sigma_g{}^{-1}+n_2\sigma_g{}^{-2}+n_3\sigma_g{}^{-3}$

[a] α_i and n_i (i=0, 1, 2, 3, ...) are fitting parameters, *S* is sand fraction, *CL* is clay fraction, *C* is carbon content, and *BD* is bulk density.

parameter n as a linear function of $\sigma_g{}^{-1}$. Recently, after an analysis by the Bayesian probabilistic method based on a database, *Chiu et al.* [2012] proposed a similar form of relationship between the parameter α and a measure of mean particle size, in which they employed d_{50}. And, they also formulated the parameter n as a function of σ_g as a polynomial function.

From the summary of the pedotransfer functions in Table 1, it can be observed that the parameter α, which is related to air entry value, is inversely proportional to a measure of mean particle size in general. The parameter n, associated with the slope of desaturation in water retention curve, is in function of a measure of grain size uniformity as the desaturation process is physically governed by the pore size distribution which has an intrinsic relationship with particle size distribution [*Feia et al.*, 2014]. This is schematically summarized in Figures 1a and 1c. For practical applications in engineering, a preliminary but straightforward estimation of water retention curve (thus capillary induced strength) from more basic soil gradation parameters on these two aspects may be interesting.

3. Estimating WRC From Soil Gradation

3.1. Theoretical Characterization

In geotechnical engineering, d_{10}, d_{30}, and d_{60} (particle sizes at 10%, 30%, and 60% passing by weight, see Figure 1c) are three important particle sizes in describing soil gradation [*Terzaghi et al.*, 1996]. The coefficient of uniformity (C_u) and the coefficient of curvature (C_c) are then expressed based on these three particle sizes as

$$C_u=\frac{d_{60}}{d_{10}} \tag{10}$$

$$C_c=\frac{(d_{30})^2}{d_{60}d_{10}} \tag{11}$$

They are also commonly used to evaluate soil gradations. These basic soil gradation parameters (d_{10}, d_{30}, and d_{60} and thus C_u and C_c) can be employed to predict soil properties such as permeability functions [*Hazen*, 1892; *Kenney et al.*, 1984], hydraulic conductivity [*Mbonimpa et al.*, 2002; *Vienken and Dietrich*, 2011] and also water retention behavior [*Aubertin et al.*, 2003]. If considering d_{60} as a measure of mean particle size of a specimen, the parameters of d_{60}, C_u, and C_c can determine the basic shape of the PSD of a granular soil.

Dimensional analysis, or Buckingham's Pi theorem [*Buckingham*, 1914], is widely used in analyzing science and engineering problems. It rewrites a physical relationship as independent and dimensionless groups of variables which may reduce the total number of variables and thus simplifies the physical relationship. When drying a sandy soil, the effective degree of saturation (S_e) relies on the PSD, suction and also the water surface tension value (noted as γ). If using C_u, C_c, and d_{60} to determine the PSD, S_e [–] can be expressed as a function (function f as below) of variables of C_u [–], C_c [–], d_{60} [L], ψ [$M\,L^{-1}\,T^{-2}$], and γ [$M\,T^{-2}$], where – means dimensionless and L, M, and T represent length, mass, and time units, respectively. By applying Buckingham's Pi theorem, all variables are written as groups of dimensionless terms. The dimensionless quantity S_e [–] is kept as the dependent variable and C_u [–] and C_c [–] are also nondimensional independent quantities. d_{60} [L], ψ [$M\,L^{-1}\,T^{-2}$], and γ [$M\,T^{-2}$] can be written as a dimensionless group of $\frac{\psi d_{60}}{\gamma}$. Therefore, the f function can be simplified as a f' function as

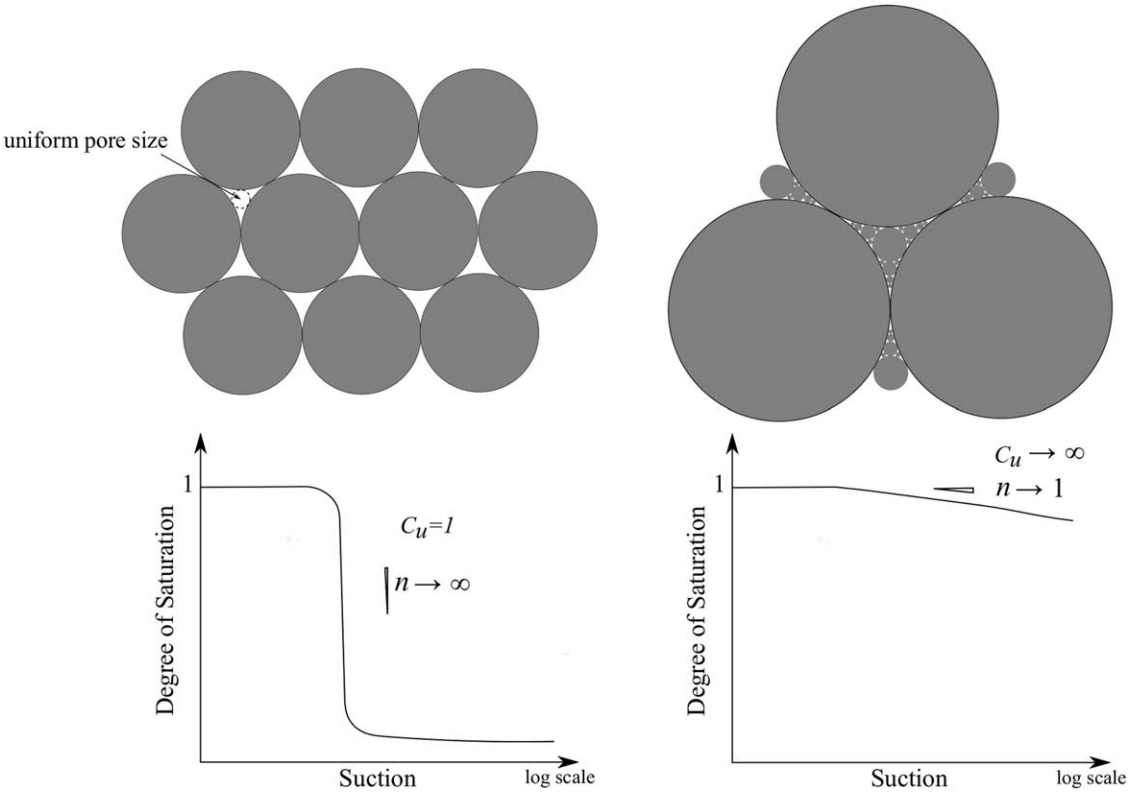

Figure 2. Two extreme scenarios at C_u=1 and $C_u \to \infty$.

$$S_e = f(C_u, C_c, d_{60}, \psi, \gamma) = f'\left(C_u, C_c, \frac{\psi d_{60}}{\gamma}\right) \tag{12}$$

For sandy soils, usually C_c is a dependent parameter on C_u (we will validate this in a later section), then the effective degree of saturation can be approximate as

$$S_e \approx f''\left(C_u, \frac{\psi d_{60}}{\gamma}\right) \tag{13}$$

Meanwhile, equation (2) can be rewritten by normalized suction ($\psi^* = \frac{\psi d_{60}}{\gamma}$) and normalized α ($\alpha^* = \frac{\alpha d_{60}}{\gamma}$) as

$$S_e = \left(1 + \left(\frac{\psi^*}{\alpha^*}\right)^n\right)^{\frac{1}{n}-1} \tag{14}$$

Considering the dimensional analysis in equation (1) that S_e is approximately only related to $\psi^* = \frac{\psi d_{60}}{\gamma}$ and C_u and also combining with the PTFs in literature, one can deduce that the parameter n can be a function of the coefficient of uniformity (C_u) and the normalized parameter $\alpha^* = \frac{\alpha d_{60}}{\gamma}$ is either related to C_u or a constant.

Here we also consider two extreme scenarios to clarify the limit values of parameter n (Figure 2). One is a monosized granular material, of which the coefficient of uniformity C_u=1. For simplification, the particles are assumed to be spheres. In this case, pores in the granular medium have a relatively narrow range in size. They can be regarded as unit cells with throats connecting them and when the suction reaches the air entry value governed by the size of the throat, most cells start to drain water out [*Or and Tuller*, 1999; *Tuller et al.*, 1999]. This leads the slope of the WRC to be very steep (thus, $n \to \infty$ in equation (2)). Another scenario is that the material is extremely polydisperse ($C_u \to \infty$). This means that all the pores are filled with finer particles which lead the soil very difficult to desaturate. Therefore, the slope of the WRC will be a rather flat shape and from equation (2) the minimum value of parameter n will be reduced and approach 1.

3.2. Experimental Tests on Nearly Monodisperse Materials

In the UNSODA database, most of the soils have relatively high C_u values so that the first extreme condition in Figure 2 cannot be covered. Before carrying out a systematic analysis of water retention behaviors of different sandy soils on the database, we first conducted a set of supplementary water retention tests on granular materials with nearly monodisperse particle size distributions. Both glass beads with rounded particle shapes and sands with irregular shapes were tested. The four types of tested glass beads were supplied by Sigmund-Lindner® and their particle size distributions are presented in Figure 3a. Four sands were also tested with one silica "Mol sand" supplied by Sibelco® and one medium sand from a construction site. Another two types of sands (sands A and B) were sieved from the medium sand which makes the particle sizes of sands A and B ranging from 0.208 to 0.417 mm and from 0.417 to 0.833 mm, respectively. The PSDs of the four sands are plotted in Figure 3b in which the data of Mol sand are from the supplier and the rest are from sieve analysis.

The determination of the water retention curves was based on a tensiometric suction control technique and a level-adjustable burette for the measurement of water volume exchange in Figure 4a (this method is also referred as the "hanging water column method") [*Dane and Hopmans*, 2002]. The sample was prepared in a circular mold with top cap opened to the atmosphere. There is a thin porous stone plate under the sample connecting with a pipe to a burette as the water reservoir. The sample was first saturated by controlling the water level in the burette as the same level of the top of the sample. Then the burette was lowered to a certain level, inducing a negative water pressure and suction. After water table stabilization, the raised water level in the burette (z_2) represents the entered air phase volume in the sample. Thus, water content (and degree of saturation) can be obtained by knowing sample volume and porosity. Suction can be measured by the level distance between water table and sample center (z_1) as $\psi = \rho g z_1$.

The measured water retention behaviors are shown in Figures 4b and 4c in symbols. The best fitted curves by the *van Genuchten's* equation (fitting errors can be seen in Appendix A) are plotted in lines. It can be observed that the *van Genuchten's* equation models the water retention behaviors very well. It can also be seen that the slope the WRC is closely associated with the slope of the PSD in Figure 3. Higher grain size polydispersity makes the soil harder to be desaturated.

3.3. Analysis of the Experimental Results and UNSODA Data

Analysis of more polydisperse materials was based on the UNSODA database [*Leij et al.*, 1996]. This database comprises 780 soils with their water retention curves and/or hydraulic conductivities data measured. For the purpose to analyze the data from a more efficient and reliable way, two aspects were considered in the soil selection. The first aspect is that the soil should have a clear particle size distribution with the smallest measured particle size less than 10% passing and the largest measured particle size beyond 60% passing. This is to obtain the d_{60} and C_u values. The second aspect is that the soil should have a water retention curve of the first drying with the residual state reached at high suction (low degree of saturation) in the

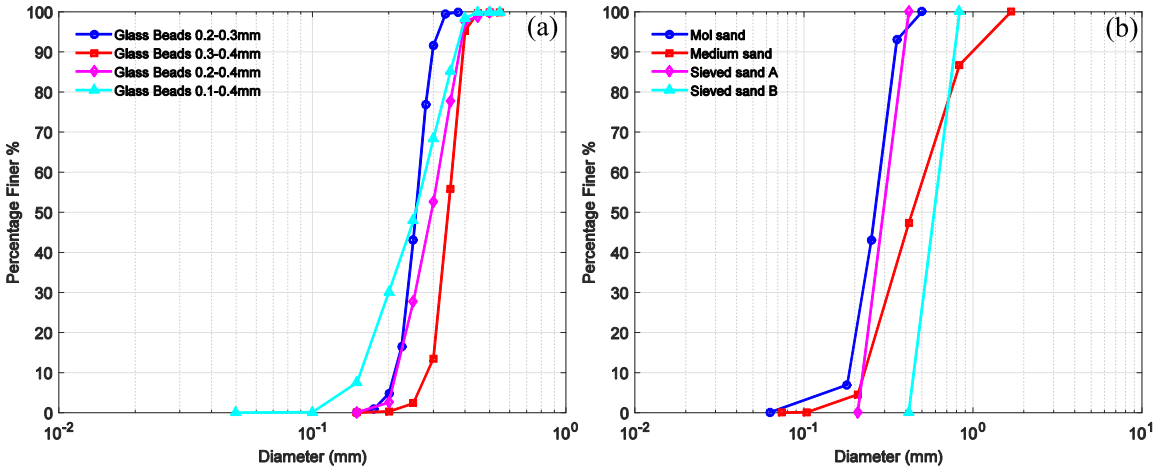

Figure 3. Particle size distributions of the tested glass beads and sands. (a) Glass beads and (b) sands.

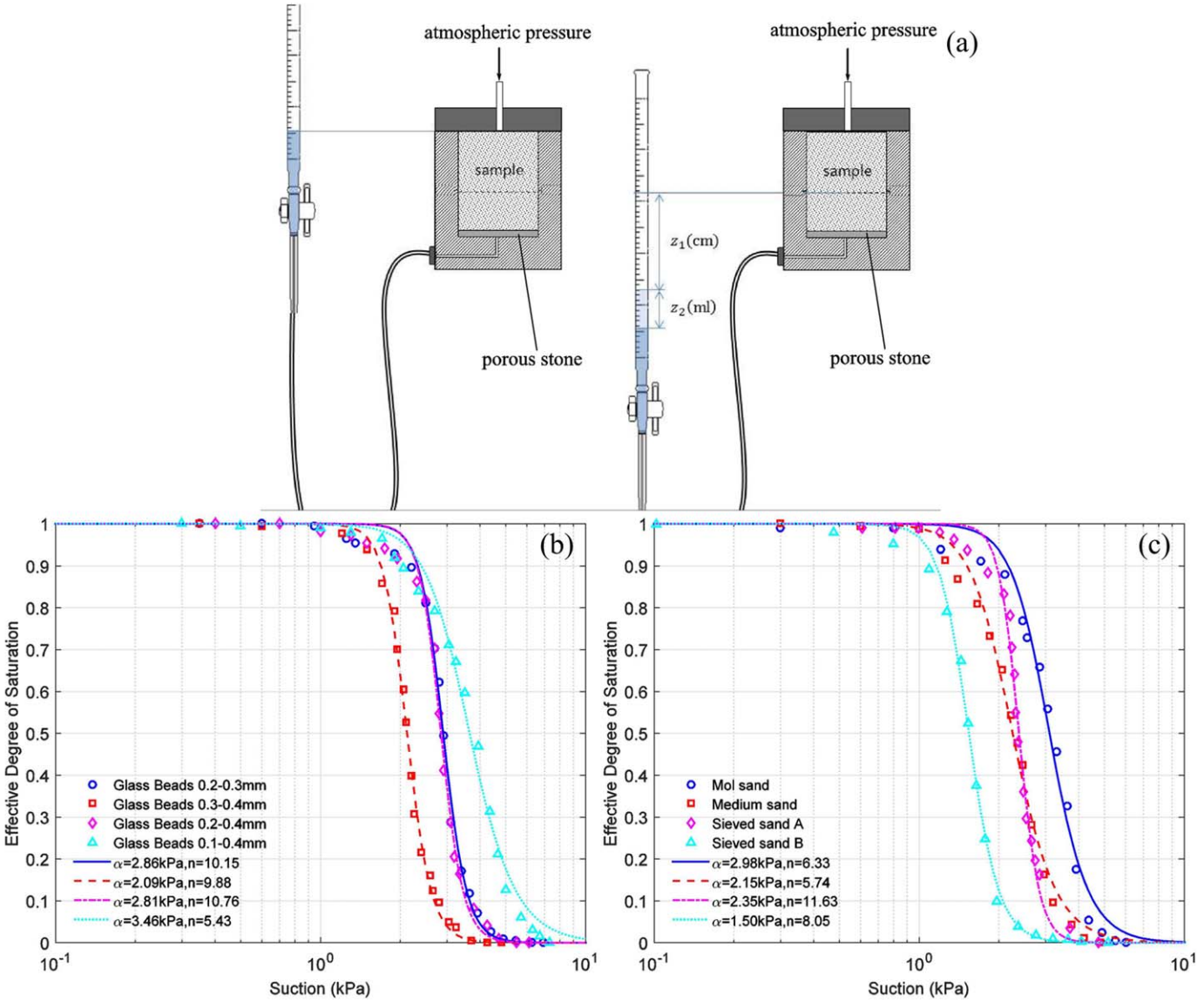

Figure 4. Water retention curve of relatively uniform sands and glass beads. (a) Measurement technique, (b) WRC of glass beads, and (c) WRC of sands.

data. A selection criterion was set as if the slope of the water retention curve of the three data points at the highest suction in the semilogarithm plot is less than 0.15 and the final degree of saturation is also less than 20% then we assume it reaches the residual state. Constrained on these two aspects a total of 70 sandy soils were selected from the database for this analysis. Sand fractions of these 70 soils are all larger than 60% and the coefficient of C_u is within 100. The water retention curves of these soils were also fitted by the *van Genuchten's* equation (equation (2)) by the least squares method and the soil IDs, soil gradation parameters, fitting parameters and fitting errors can be seen in Appendix A. The soil gradation parameters of d_{10}, d_{30}, d_{60}, . . . were obtained from the semilogarithm PSD curve by interpolation, which was done by a customized Matlab code.

The analysis on the relationship between soil gradation parameters and water retention parameters could then be conducted on the data of the 8 tested granular materials and the chosen 70 soils from the UNSODA database. As in equation (13), the parameter C_c is assumed to be associated with C_u, a validation is carried out in Figure 5a in which the relationship between these two parameters of the studied soils is plotted in a logarithm sketch. It can be seen that the C_c has a clear dependent relationship with C_u, which verifies the assumption.

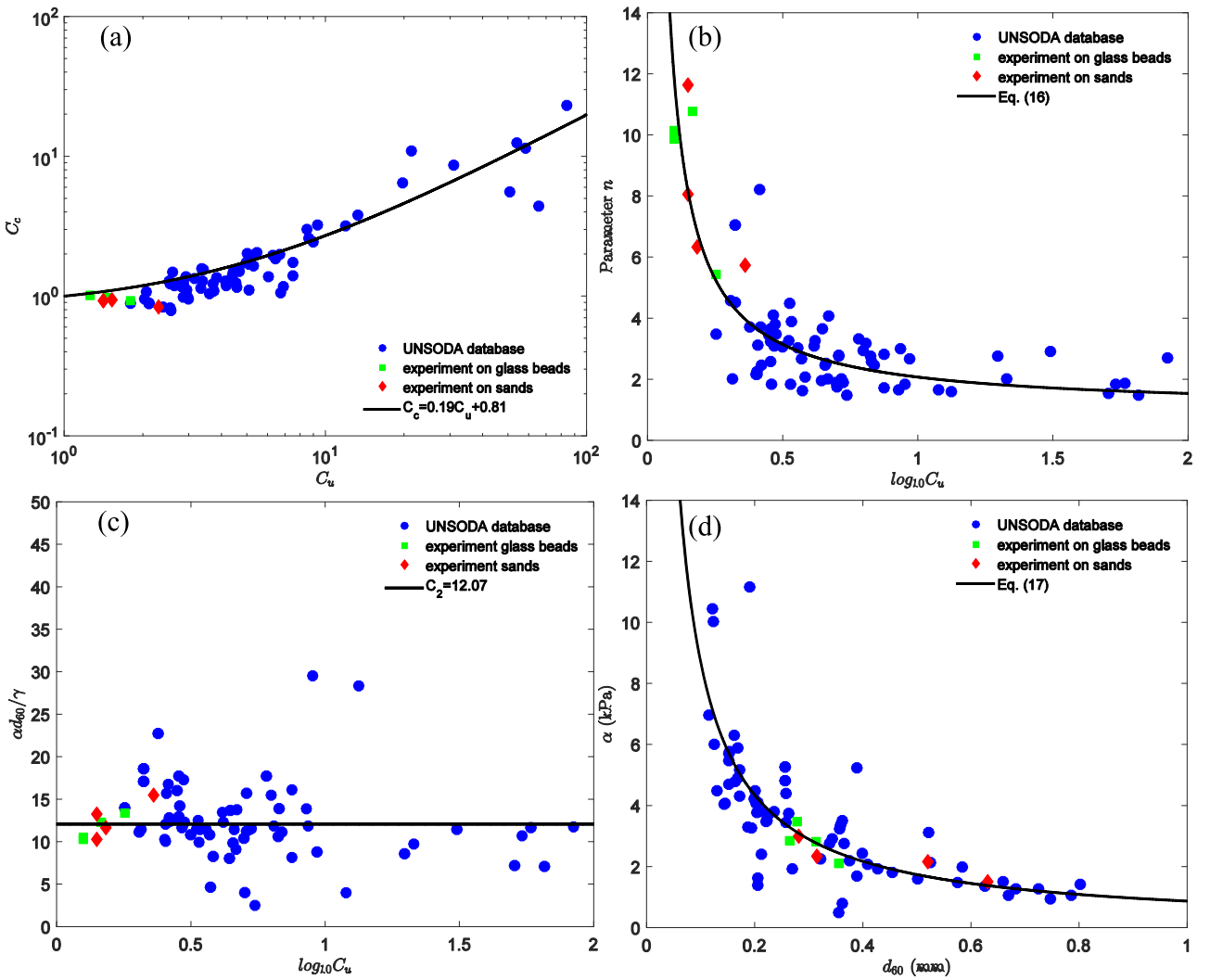

Figure 5. Modeling of parameters for WRC: (a) correlation between C_c and C_u, (b) modeling of parameter n, (c) modeling of normalized α against C_u, and (d) modeling of α against d_{60}.

The slope of a PSD in a semilogarithm plot may be simply quantified by

$$\text{PSD slope} \approx \frac{0.01(y-x)}{\log_{10}(d_y)-\log_{10}(d_x)} = \frac{0.01(y-x)}{\log_{10}\left(\frac{d_y}{d_x}\right)} \tag{15}$$

where d_x and d_y are two characteristic particle sizes at x% and y% passing, respectively. If using the parameter $C_u = {}^{d_{60}}/_{d_{10}}$ to quantify the slope then it equals to $\frac{0.5}{\log_{10}(C_u)}$. In Figure 5b, the best fitted n parameter of the 8 tested granular materials and the 70 sandy soils from the UNSODA database are plotted against $\log_{10}(C_u)$. It satisfies the conditions discussed in Figure 2 that when C_u approaches 1 the parameter n tends to be infinite and when C_u is very high the parameter n decreases to about 1. The following type of equation can be employed to fit the n and $\log_{10}(C_u)$ relationship:

$$n = \frac{C_1}{\log_{10}(C_u)} + 1 \tag{16}$$

where C_1 is a fitting parameter by the least squares method such that $C_1 \approx 1.07$.

After the dimensional analysis in the previous section, the normalized parameter $\alpha^* = \frac{\alpha d_{60}}{\gamma}$ is believed to be either related to C_u or to be a constant. Figure 5c presents the values of $\frac{\alpha d_{60}}{\gamma}$ of materials with different C_u. The correlation between $\frac{\alpha d_{60}}{\gamma}$ and C_u is not obvious which means that the normalized α could be

independent to C_u. Therefore, it is assumed that $\frac{\alpha d_{60}}{\gamma}$ is approximately a constant C_2 which means α is inversely proportional to the mean particle size as other authors already introduced in Table 1. That yields

$$\alpha = \frac{C_2 \gamma}{d_{60}} \tag{17}$$

The correlation between α and d_{60} is depicted in Figure 5d. C_2 is fitted to be 12.07 by the 78 samples. In the basic assumptions, the void ratio variation is assumed to be small and the grain shape angularity is not considered. The scatters and errors in Figures 5b and 5c could be induced by these two aspects. These two aspects could be worthwhile to be considered in future studies.

3.4. Validation of the Model

Validation of equations (16) and (17) can be carried out by comparing the estimated n and α values with the measured ones on the 8 tested materials and the 70 soils from the database (in Figures 6e and 6f). In Table 1, PTFs are proposed by *Schaap and Bouten* [1996] by using neural network and the PTFs of *Chiu et al.* [2012] are based on the Bayesian probabilistic method. Our predictions are compared with the predictions of these two models in Figures 6a–6d to evaluate the accuracy of the proposed method. It should be noted that the fitting parameters used in the models of *Schaap and Bouten* [1996] and *Chiu et al.* [2012] are best fitted ones on the 78 materials with the least squares method other than the ones in their model development as the materials used are not entirely the same. This leads the comparison on a fairer basis. Statistical parameters of the root-mean-square error (RMSE), the sum of square errors (SSE), and the coefficient of determination (R^2) of the different predictions are calculated and their values are also demonstrated in the figure. For the prediction of the parameter n, it can be seen that the expression of equation (16) is much better than the models of *Schaap and Bouten* [1996] and *Chiu et al.* [2012], as it has lower errors and a higher coefficient of determination. The prediction of n is especially improved for the materials we tested with relatively narrow PSDs, which shows the necessity of the theoretical consideration of a monosize packing. A model combining the key physical features and statistical analysis has a better prediction than that from a pure regression analysis. For predicting the parameter α, all models have fair results as they have similar prediction errors and our model and *Chiu's* are slightly better. Since d_{60} is already required for calculating C_u, the model in equation (17) has better simplicity without measuring an additional parameter d_p or d_{50}.

In equation (16), the effect of PSD slope is quantified by C_u, which means the slope is quantified by d_{10} and d_{60}. It may be possible to use other combinations of characteristic particle sizes (d_x and d_y in equation (15)) to describe the PSD slope. The results of replacing C_u in equation (16) by other combinations are introduced in Table 2. d_{10}, d_{20}, and d_{30} are adopted as the d_x value, respectively, and d_{60}, d_{70}, d_{80}, and d_{90} are used as the d_x value, correspondingly. By replacing C_u as d_y/d_x, corresponding C_1 values are obtained statistically (with least squares errors) from the 78 materials. The accuracy is quantified by statistical parameters of RMSE, SSE, and R^2. It can be seen that using d_{10} as d_x generally has a better fitness than using d_{20} and d_{30}. It can be seen that using C_u, saying d_{60}/d_{10}, has the best results. Although d_{90}/d_{10} has similar goodness of fitting, C_u is a more commonly available parameter for geomaterials and prediction from C_u is more convenient.

Now it is necessary to check the applicability of the model to soils beyond the database. Six soils mainly composed by sands are selected from literature [*Fredlund et al.*, 1997; *Yang et al.*, 2004; *Gallage and Uchimura*, 2010] for validation. The PSDs of the six soils are depicted in Figure 7a which shows different mean particle sizes and uniformities. For the fine sand and the loamy sand from *Fredlund et al.* [1997], they have similar d_{60} but quite different C_u as measured from the PSD chart. The parameters of n and α are predicted by equations (16) and (17) and then can be substituted into equation (2) to obtain the WRC. In Figure 7b, the measured WRC in first drying from fully saturated state (plotted as symbols) are compared with the predicted WRC (lines). It can be seen that, for the fine sand, which has a lower C_u value, the prediction matches well with the experimental data. For the loamy sand, the estimation shows some errors in the high suction range due to the uncertainty of the value of the residual degree of saturation. Similar comparisons are made for the soils from *Yang et al.* [2004] and *Gallage and Uchimura* [2010] in Figures 7c and 7d. It can be seen that the proposed model generally has a good prediction on these soils. In the clayey sand and the Chiba soil, it shows some underestimation in the low suction range. These are from two aspects: for soils with very low d_{10} it becomes more difficult to determine the residual state; and as the void ratio and fabric

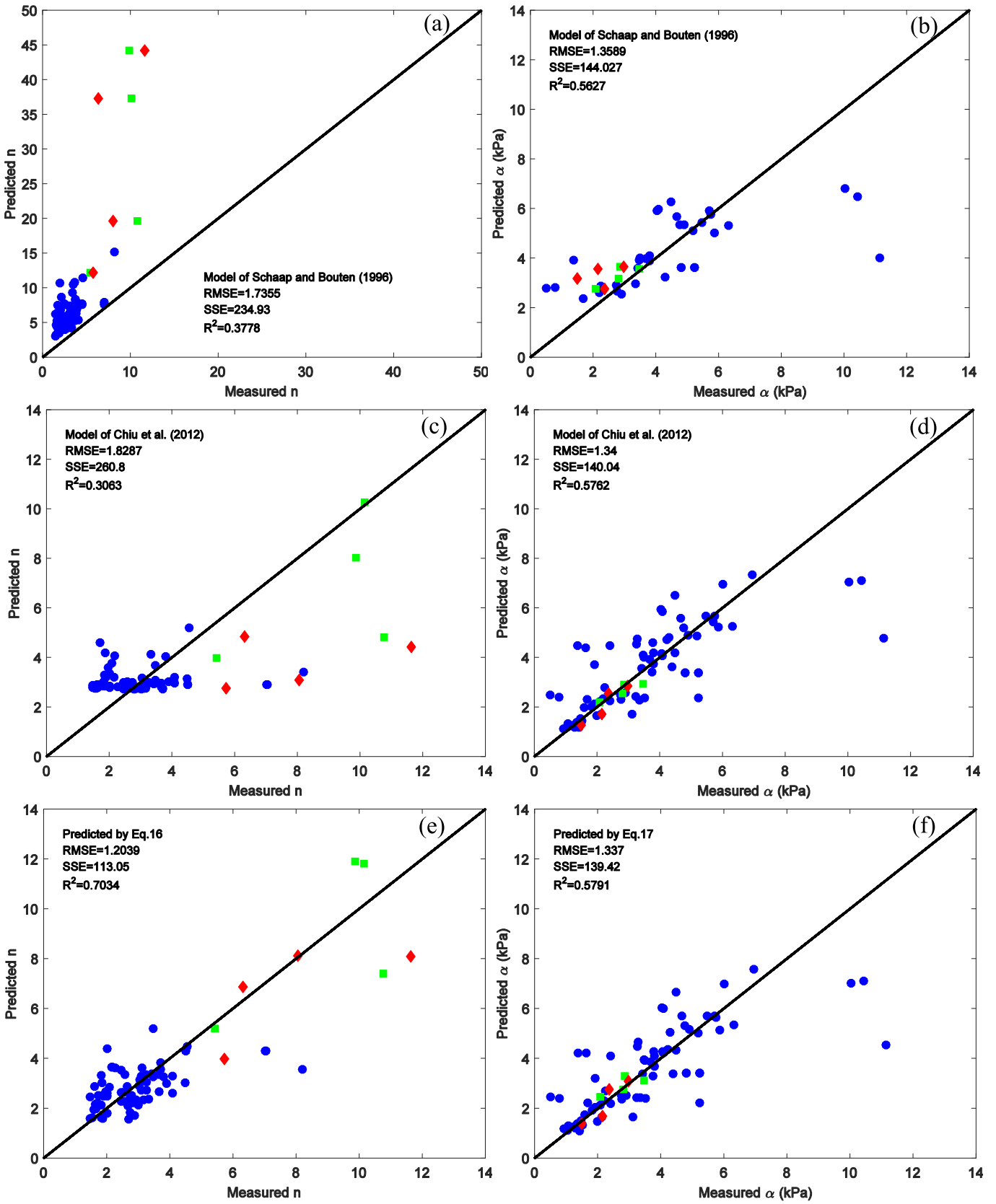

Figure 6. Comparisons between model predictions and experiment measurements: (a) prediction of n by the model of *Schaap and Bouten* [1996], (b) prediction of α by the model of *Schaap and Bouten* [1996], (c) prediction of n by the model of *Chiu et al.* [2012], (d) prediction of α by the model of *Chiu et al.* [2012], (e) prediction of n by equation (16), and (f) prediction of α by equation (17).

Table 2. Predictions of Parameter *n* by Using Different Combinations of Characteristic Particle Sizes

	$\frac{d_{60}}{d_{10}}$	$\frac{d_{70}}{d_{10}}$	$\frac{d_{80}}{d_{10}}$	$\frac{d_{90}}{d_{10}}$	$\frac{d_{60}}{d_{20}}$	$\frac{d_{70}}{d_{20}}$	$\frac{d_{80}}{d_{20}}$	$\frac{d_{90}}{d_{20}}$	$\frac{d_{60}}{d_{30}}$	$\frac{d_{70}}{d_{30}}$	$\frac{d_{80}}{d_{30}}$	$\frac{d_{90}}{d_{30}}$
C_1	1.07	1.26	1.45	1.69	0.571	0.867	1.054	1.287	0.492	0.649	0.832	1.068
RMSE	1.204	1.232	1.234	1.205	1.332	1.359	1.341	1.294	1.409	1.433	1.409	1.335
SSE	113.05	118.42	118.82	113.17	138.46	144.05	140.29	130.63	154.73	160.22	154.93	138.97
R^2	0.7034	0.6876	0.6862	0.7025	0.6319	0.617	0.627	0.653	0.5935	0.5768	0.5896	0.6304

effects are not considered in this model, there may be an error in estimating the air entry value when clay fraction is higher. Nevertheless, this models shows fair predictions on different soils and may be a useful model for estimating water retention behaviors from just two basic soils gradation parameters (d_{10} and C_u).

4. Coupling PTFs With Material Strength

4.1. Relationship Between PSD and Strength

As introduced in section 2.2, the material strength of an unsaturated soil is intrinsically correlated with its water retention behavior. By using the *van Genuchten's* WRC model to formulate the relationship between suction and effective degree of saturation, it gives great convenience to embed the PTFs into the shear

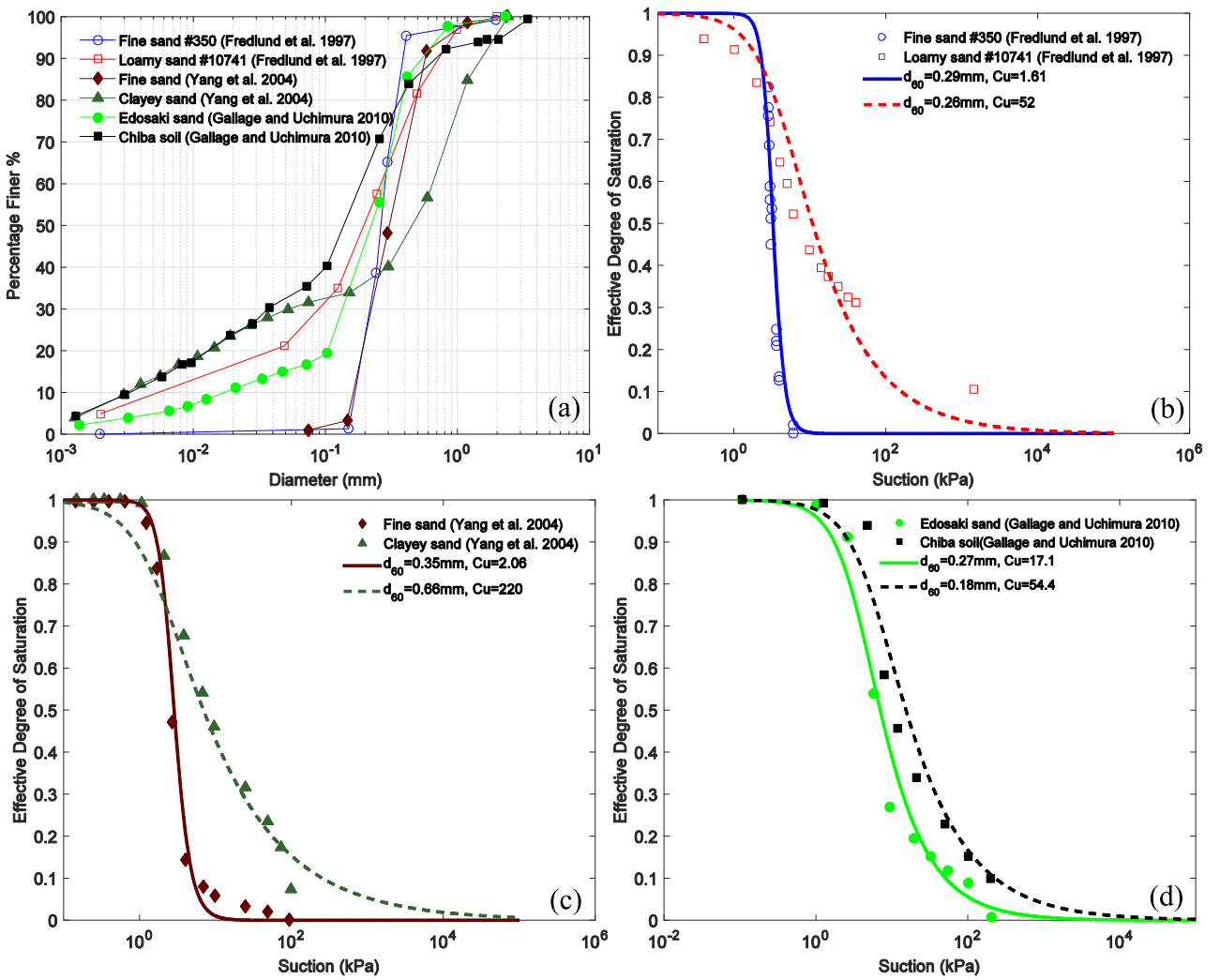

Figure 7. Validation of the model for soils beyond the studied samples. (a) PSD of the soils for validation, (b) validation of samples from *Fredlund et al.* [1997], (c) validation of samples from *Yang et al.* [2004], and (d) validation of samples from *Gallage and Uchimura* [2010].

strength criteria based on *Lu*'s suction stress concept. First, the WRC equation in equation (2) can be substituted into equation (6). The shear strength can be expressed in function of suction as

$$\tau=(\sigma-u_a)\tan\phi+\left[1+\left(\frac{u_a-u_w}{\alpha}\right)^n\right]^{\frac{1-n}{n}}(u_a-u_w)\tan\phi \tag{18}$$

or, as a function of the effective degree of saturation as

$$\tau=(\sigma-u_a)\tan\phi+\alpha S_e\left(S_e^{\frac{n}{1-n}}-1\right)^{\frac{1}{n}}\tan\phi \tag{19}$$

Without considering hydraulic history, by substituting the proposed PTFs of equations (16) and (17) into the above two equations, the shear strength of an unsaturated sandy soil can be estimated by using the net stress $(\sigma-u_a)$, the internal friction angle, the key particle size distribution parameters (d_{60} and C_u) and suction or effective degree of saturation as

$$\tau=(\sigma-u_a)\tan\phi+\left[1+\left(\frac{d_{60}(u_a-u_w)}{C_2\gamma}\right)^{\frac{C_1}{\log_{10}(C_u)}+1}\right]^{\frac{-C_1}{C_1+\log_{10}(C_u)}}(u_a-u_w)\tan\phi \tag{20}$$

and

$$\tau=(\sigma-u_a)\tan\phi+\frac{C_2\gamma}{d_{60}}S_e\left(S_e^{-\frac{C_1+\log_{10}(C_u)}{C_1}}-1\right)^{\frac{\log_{10}(C_u)}{C_1+\log_{10}(C_u)}}\tan\phi \tag{21}$$

The parameters C_1 and C_2, according the statistical analysis in the previous section, are approximated as 1.07 and 12.07, respectively. The water surface tension γ depends on temperature and salinity, as a reference, for distilled water at 20°C, $\gamma = 0.073$ N/m.

4.2. Particle Size Effect on Suction Stress

According to *Lu and Likos* [2006] and *Lu et al*. [2010], the suction stress of an unsaturated soil can be evaluated by its tensile strength. If the Mohr-Coulomb failure criterion is applied, the uniaxial tensile strength (as $\sigma_t=-\sigma_1$ and $\sigma_3=0$) has the following relationship with suction stress:

$$\sigma_t=-2\tan\phi\tan\left(\frac{\pi}{4}+\frac{\phi}{2}\right)\sigma_s=2\tan\phi\tan\left(\frac{\pi}{4}+\frac{\phi}{2}\right)S_e(u_a-u_a) \tag{22}$$

where ϕ is the internal friction angle. Considering the relationship between PSD and WRC, the tensile strength yields

$$\sigma_t=2\tan\phi\tan\left(\frac{\pi}{4}+\frac{\phi}{2}\right)\left[1+\left(\frac{d_{60}(u_a-u_w)}{C_2\gamma}\right)^{\frac{C_1}{\log_{10}(C_u)}+1}\right]^{\frac{-C_1}{C_1+\log_{10}(C_u)}}(u_a-u_w) \tag{23}$$

In *Lu et al*. [2010], the closed-form suction stress definition in granular soils is corroborated by the tensile strength of a limestone agglomerate [*Schubert*, 1984] and an Ottawa sand [*Kim and Sture*, 2008]. Here the same set of data can be used to verify the estimation from the PSD parameters. The limestone agglomerate is a nearly monodisperse material with a mean particle size of 0.071 mm, for which d_{60} and C_u can be estimated as 0.071 mm and 1.1, respectively. The Ottawa sand is a commercially available sand with $d_{60} = 0.24$ mm and $C_u = 2$. Then by equations (16) and (17), the WRCs of these two granular materials can be estimated. In Figure 8a, the predicted curves are plotted with the experiment results (in scatters). It can be seen that they have a good agreement with each other. The internal friction angle of the Ottawa sand is measured as 36° as reported by *Baltodano-Goulding* [2006]. For the limestone agglomerate, which is a finer and denser material, the friction angle is approximated as 40°. By substituting the particle size parameters and the friction angles into equation (27), the tensile strength of the two materials can be estimated and in Figure 8b the predicted values are compared with the measured data. The estimation errors may be due to measurement error on friction angle or the change of friction angle in the tensile range and may also come from the errors in estimating the air entry value. Nevertheless, the quantitative trend of the prediction agrees with the experimental results.

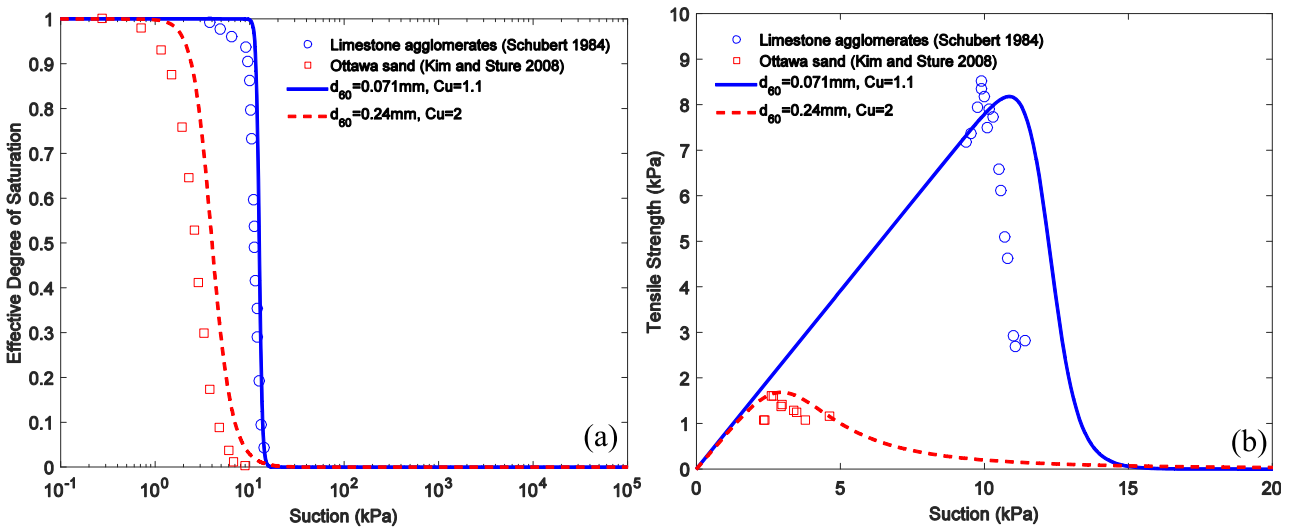

Figure 8. From d_{60} and C_u to tensile strength. (a) Estimation of WRC and (b) estimation of tensile strength.

4.3. Particle Size Effect on Capillary Cohesion

Furthermore, the capillary effect induced cohesion of a granular soil (in direct shear test or triaxial test) can also be quantitatively estimated from the basic PSD parameters. For sandy soils, the interparticle van der Waals attraction and double-layer electronic effect are negligible. Therefore, the cohesion in unsaturated sandy soils is mainly due to the capillary effect. From equations (6) and (19), the capillary cohesion can be expressed as

$$c_{cap}=S_e(u_a-u_a)\tan\phi=\alpha S_e\left(S_e^{\frac{n}{1-n}}-1\right)^{\frac{1}{n}}\tan\phi \tag{24}$$

Focusing on the PSD effect and degree of saturation effect, from equation (21), the cohesion is

$$c_{cap}=\frac{C_2\gamma'}{d_{60}}S_e\left(S_e^{-\frac{C_1+\log_{10}(C_u)}{C_1}}-1\right)^{\frac{\log_{10}(C_u)}{C_1+\log_{10}(C_u)}}\tan\phi \tag{25}$$

It can be seen from the above equation that at the same degree of saturation, the capillary cohesion is inversely proportional to the soil main grain size (quantified by d_{60} in the equation).

The estimated trends of capillary cohesion of sandy soils with various PSDs can be quantitatively compared with experimental measurements based on direct shear tests or triaxial tests performed at different controlled suctions in the literature [*Gallage and Uchimura*, 2006; *Hossain and Yin*, 2010; *Likos et al.*, 2010]. Figure 9 presents the estimated WRC and capillary cohesion (in lines) as well as the measured data (in symbols).

Hossain and Yin [2010] tested a granite soil with d_{60} = 0.11 mm and C_u = 90. As the C_u is relatively large, the soil is more difficult to be desaturated and by fitting with the *van Genuchten*'s model, its residual degree of saturation is high ($S_r^r \approx 45\%$). The material was sheared at certain suction levels on the drying path with different normal stresses. The average friction angle is about 38° and the capillary cohesion is obtained from the Mohr-Coulomb lines. Experimental results are available for relatively high suction levels, far away from the air entry suction. For this material, capillary cohesion still increases with suction, even at low effective degree of saturation. This trend is well reproduced by the model.

Edosaki sand (d_{60} = 0.27 mm, C_u = 17) was tested by *Gallage and Uchimura* [2006] in a suction controlled triaxial apparatus. The average friction angle is about 46.2° and capillary cohesion values at different suctions on the drying path are selected for comparison. The PTFs show good prediction on the water retention behavior and the estimated capillary cohesion trend coincides with the measured data. As the Edosaki sand has a larger mean grain size and lower grain size polydispersity, its capillary cohesion value is much smaller than that of the granite soil.

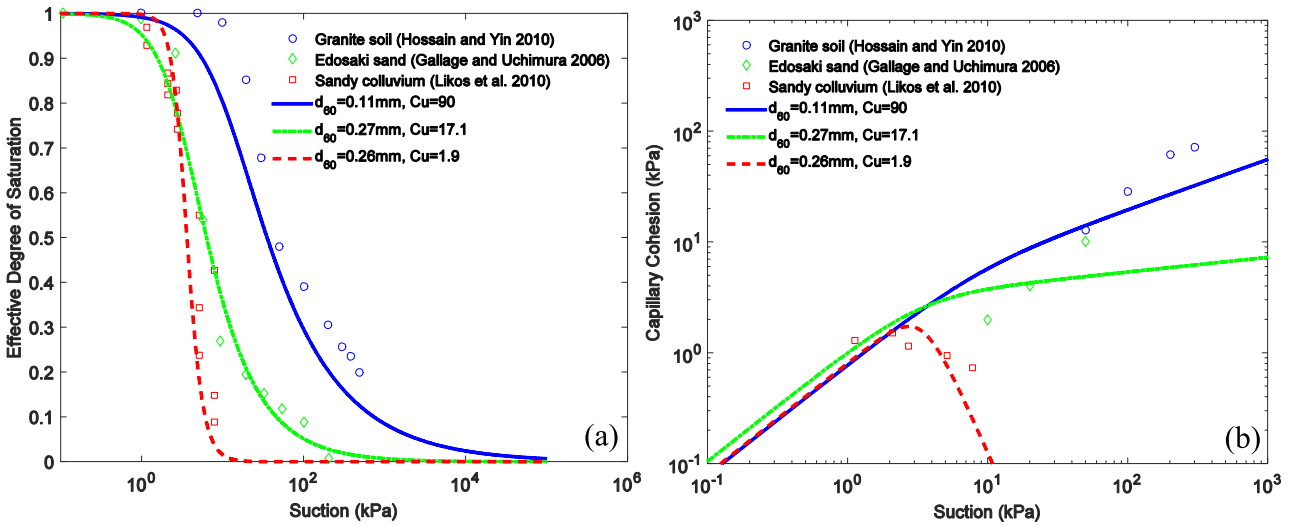

Figure 9. From d_{60} and C_u to capillary cohesion. (a) Estimation of WRC and (b) estimation of capillary cohesion.

Likos et al. [2010] developed a direct shear apparatus for low suction and low stress conditions. A sandy colluvium ($d_{60} = 0.26$ mm, $C_u = 1.9$) was tested with different suction values. It has a similar mean grain size comparing to the Edosaki sand but the grain size range is much narrower. The friction angle of this material is about 38.8°. We take the shear test results under the lowest normal stress (0.33 kPa) to evaluate the capillary cohesion. After air entry value, there is a peak capillary cohesion value existing. Beyond that further decrease in water content also reduces the cohesion. Overall, the experimental results qualitatively confirm the estimation from soil gradation. The peak of capillary cohesion is well reproduced by the model.

It can be seen from Figure 9b that there may be a maximum cohesion value at a certain degree of saturation for clean sands. Taking the derivative of equation (24) with respect to S_e and then equal that derivative to 0, the S_e value at the maximum cohesion can be obtained:

$$(S_e)_{\max} = \left(\frac{1-n}{2-n}\right)^{(1-n)/n} \tag{26}$$

Substituting it into equation (24), the maximum cohesion is

$$c_{\max} = \alpha\left(\frac{1-n}{2-n}\right)^{\frac{1-n}{n}}\left(\frac{1}{n-2}\right)^{\frac{1}{n}}\tan\phi \tag{27}$$

Furthermore, by considering the PSD effect with the developed PTF in equations (16) and (17), the maximum cohesion can be estimated by the equivalent mean particle size d_{60}, particle size uniformity C_u, internal friction angle ϕ and other material constants as

$$c_{\max} = \frac{C_2\gamma}{d_{60}}\left(\frac{C_1}{C_1-\log_{10}(C_u)}\right)^{\frac{-C_1}{C_1+\log_{10}(C_u)}}\left(\frac{\log_{10}(C_u)}{C_1-\log_{10}(C_u)}\right)^{\frac{\log_{10}(C_u)}{C_1+\log_{10}(C_u)}}\tan\phi \tag{28}$$

From equation (26), a maximum cohesion only exists when $n > 2$. This means $C_u < 11$ if $C_1 = 1.07$. This can be confirmed by the experimental observation in Figure 9b that cohesion of the Edosaki sand ($C_u > 11$) monotonically increases with suction and the sandy colluvium ($C_u < 11$) has a peak capillary cohesion value.

The mean particle size and particle size uniformity effects on capillary cohesion can be theoretically characterized. Figure 10 demonstrates typical theoretical solutions of WRCs and cohesions from the two basic PSD parameters (the internal friction angle ϕ is assumed to be a typical value of 35°). First, the d_{60} size is assumed to be 0.2 mm and three different values of C_u (2, 10, and 50) are applied which means the materials can be categorized from clean fine sand to silty or clayey sand. The theoretical solutions of WRCs and the corresponding cohesion in function of effective degree of saturation are then plotted in Figures 10a and 10c by the developed PTFs and equation (25). For a same d_{60}, with the increase of C_u, the maximum suction the material

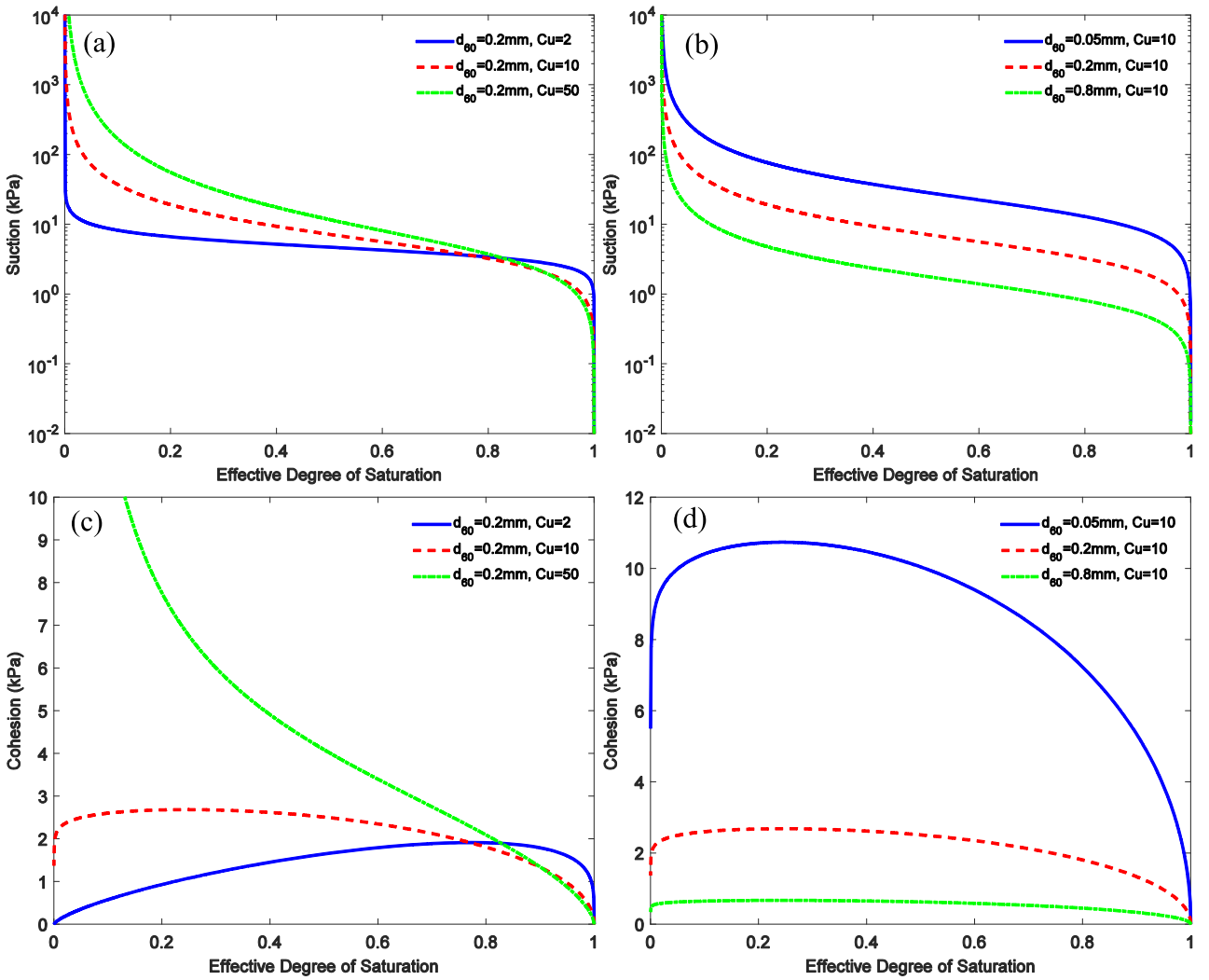

Figure 10. Theoretical solutions of PSD effect on WRC and capillary cohesion. (a) Effect of C_u on WRC, (b) effect of d_{60} on WRC, (c) effect of C_u on capillary cohesion, and (d) effect of d_{60} on capillary cohesion.

can reach (drying to a very low water content) is significantly increased. Subsequently, the cohesion at a relatively low degree of saturation is also increased. For a soil with a fraction of silt or clay particles ($C_u > 11$), there is no obvious maximum value, and the cohesion tends to be very large when the water content is relatively low. Furthermore, with a same C_u, by increasing the equivalent mean particle size (d_{60}), the PSD curve will have a parallel shift and the WRC is also a parallel shift as the air entry value decrease with mean particle size increase (Figure 10c). The maximum cohesion is inversely proportional to the mean particle size (Figure 10d).

5. Summary and Conclusions

Basic soil gradation parameters of d_{60}, as a measure of mean particle size, and the coefficient of uniformity C_u, as a measure of particle size polydispersity, are employed to estimate the WRCs of unsaturated granular soils. Two extreme scenarios of particle size uniformity are considered as physical supplementary features of the pure statistical approach. By applying dimensional analysis and regression analysis on 8 tested granular materials and 70 soils from the UNSODA database, new PTFs are proposed to estimate the WRC from the basic soil gradation parameters. Furthermore, by incorporating with the suction stress definition, the proposed PTFs are embedded in the shear strength equations which can provide a preliminary insight into the relationship between basic particle gradation parameters and soil strength for unsaturated soils. Main conclusions can be summarized as follows:

1. The semiempirical and semiphysical approach, in which basic physical characteristics are considered and the dimensional analysis method is applied, benefits the development of new PTFs which revealed the relationship between WRC and PSD. The *van Genuchten*'s model parameter α, related to air entry value, is inversely proportional to d_{60} and the parameter n, related to the slope of WRC, is inversely proportional to logarithm C_u.
2. From validations of the model by comparing the predictions with experimental measurements, it shows that although with basic parameters, the new PTFs presents better prediction performance than the previous models for sandy soils.
3. From the theoretical characterizations and its connection with classic strength theory for unsaturated soils, the water induced strength is not only related to the soil water retention behavior but also intrinsically coupled with the soil gradation. Formulations for strength of unsaturated sandy soils are derived from the parameters of d_{60} and C_u.
4. A comparison with experimental results in literature shows the estimation method for capillary cohesion has a fair agreement. The coupled theory explains the capillary effect is more significant for finer materials (equation (28)). For materials with higher particle size polydispersity, the capillary cohesion at the same degree of saturation is generally larger than that of a more uniform material.

The advantage of this estimation approach is that the parameters can be easily determined using simple tests and the formulations are established in a simple way which can be practically applied in the early stage of engineering. However, it should be noted that this approach is more suitable for sandy soils (sand fraction $>60\%$ and $C_u < 100$) as void ratio variation is assumed to be small. To consider the fabric change is essential to extend the study on soils with more clay fraction. Furthermore, the hysteresis effect of hydraulic cycles needs to be investigated in the future. In this study, *Lu*'s suction stress definition is employed with convenience in formula derivation. However, the effective stress definition for unsaturated soils is still a controversial topic. For instance, obvious capillary cohesion may still exist with a very small amount of water for granular materials [*Scheel et al.*, 2008] which may be within the residual state. Further development in effective stress theory for unsaturated soils will also benefit the strength estimation based on soil gradation parameters.

Appendix A

The soil gradation and water retention curve parameters of the analyzed samples are summarized in Table A1.

Table A1. Soil Gradation Parameters and Best Fitted WRC Parameters of α and n for the 8 Tested Materials and the 70 Soils From the UNSODA Database[a]

					Fitted Parameters		Goodness of Fitting		
Sample ID[b]	d_{10} (mm)	d_{30} (mm)	d_{60} (mm)	C_u	α (kPa)	n	SSE	RMSE	R^2
Glass beads 0.2–0.3 mm	0.211	0.237	0.265	1.256	2.859	10.145	0.0147	0.0286	0.9956
Glass beads 0.3–0.4 mm	0.283	0.319	0.355	1.253	2.089	9.876	0.0120	0.0258	0.9957
Glass beads 0.2–0.4 mm	0.214	0.254	0.314	1.470	2.813	10.759	0.0209	0.0341	0.9934
Glass beads 0.1–0.4 mm	0.155	0.200	0.278	1.799	3.461	5.433	0.0297	0.0406	0.9895
Mol sand	0.185	0.222	0.282	1.522	2.983	6.327	0.0271	0.0425	0.9887
Sieved sand A	0.223	0.256	0.316	1.416	2.353	11.631	0.0278	0.0383	0.9889
Sieved sand B	0.447	0.513	0.632	1.413	1.505	8.051	0.0093	0.0258	0.9963
Medium sand	0.227	0.314	0.521	2.293	2.147	5.739	0.0173	0.0339	0.9922
1011	0.009	0.107	0.187	19.743	3.285	2.751	0.0156	0.0472	0.9887
1014	0.021	0.115	0.194	9.350	3.250	2.662	0.0066	0.0270	0.9949
1022	0.035	0.536	0.748	21.269	0.933	2.020	0.0056	0.0265	0.9954
1030	0.004	0.098	0.204	54.058	3.771	1.833	0.0362	0.0634	0.9654
1031	0.003	0.089	0.199	58.313	4.223	1.870	0.0339	0.0614	0.9686
1041	0.059	0.137	0.203	3.420	4.066	3.889	0.0022	0.0149	0.9987
1042	0.071	0.142	0.206	2.919	4.082	4.085	0.0016	0.0126	0.9991
1043	0.060	0.137	0.201	3.367	4.482	4.471	0.0024	0.0155	0.9987
1050	0.084	0.294	0.525	6.266	2.126	2.923	0.0151	0.0355	0.9919
1051	0.007	0.304	0.576	83.972	1.467	2.690	0.0106	0.0363	0.9925
1052	0.073	0.343	0.627	8.618	1.359	3.001	0.0131	0.0330	0.9925
1053	0.232	0.420	0.683	2.941	1.254	3.097	0.0246	0.0452	0.9852
1054	0.277	0.497	0.724	2.616	1.275	3.711	0.0163	0.0368	0.9907
1060	0.096	0.221	0.399	4.150	2.419	3.095	0.0091	0.0275	0.9955
1061	0.064	0.219	0.409	6.428	2.080	3.164	0.0144	0.0346	0.9925
1062	0.014	0.225	0.428	31.018	1.929	2.894	0.0094	0.0280	0.9949

Table A1. (continued)

Sample ID[b]	d_{10} (mm)	d_{30} (mm)	d_{60} (mm)	C_u	Fitted Parameters α (kPa)	Fitted Parameters n	Goodness of Fitting SSE	Goodness of Fitting RMSE	Goodness of Fitting R^2
1063	0.126	0.244	0.454	3.610	1.815	3.019	0.0152	0.0356	0.9917
1070	0.073	0.207	0.501	6.874	1.595	2.461	0.0047	0.0198	0.9973
1071	0.078	0.252	0.585	7.488	1.987	2.816	0.0069	0.0240	0.9964
1072	0.098	0.262	0.659	6.724	1.514	2.575	0.0057	0.0218	0.9967
1073	0.158	0.375	0.802	5.081	1.414	2.790	0.0082	0.0262	0.9953
1074	0.172	0.396	0.785	4.567	1.052	2.521	0.0032	0.0163	0.998
1075	0.148	0.350	0.670	4.545	1.059	2.453	0.0117	0.0312	0.9925
1090	0.005	0.089	0.270	50.935	1.917	1.533	0.0112	0.0293	0.9912
1130	0.003	0.055	0.212	65.728	2.401	1.475	0.0172	0.0363	0.9814
1140	0.059	0.153	0.263	4.421	3.753	3.658	0.0113	0.0307	0.9949
1461	0.218	0.309	0.523	2.395	3.123	3.702	0.0503	0.0848	0.9328
1462	0.127	0.230	0.358	2.818	3.233	3.425	0.0366	0.0677	0.9548
1463	0.127	0.239	0.362	2.846	3.514	3.653	0.0251	0.0560	0.9704
1464	0.101	0.144	0.257	2.552	4.386	3.127	0.0486	0.0779	0.9502
1465	0.025	0.074	0.125	5.000	6.012	1.881	0.0048	0.0246	0.9956
1466	0.056	0.079	0.115	2.034	6.960	4.560	0.0095	0.0344	0.9934
1467	0.029	0.209	0.390	13.299	5.243	1.584	0.0107	0.0365	0.9893
2100	0.055	0.111	0.206	3.749	1.627	1.616	0.0018	0.0213	0.9977
2104	0.017	0.106	0.206	11.985	1.381	1.661	0.0030	0.0273	0.9962
3142	0.060	0.128	0.222	3.716	3.493	2.653	0.0126	0.0375	0.9902
3143	0.068	0.132	0.225	3.328	3.687	3.269	0.0059	0.0257	0.9958
3144	0.083	0.139	0.237	2.862	3.800	3.236	0.0039	0.0207	0.9973
3153	0.033	0.120	0.221	6.673	3.466	2.753	0.0091	0.0319	0.9930
3154	0.041	0.122	0.212	5.109	3.800	2.745	0.0038	0.0205	0.9971
3155	0.062	0.137	0.257	4.177	3.430	3.261	0.0072	0.0282	0.9948
3163	0.051	0.087	0.154	2.993	5.761	3.465	0.0124	0.0322	0.9935
3175	0.137	0.271	0.358	2.610	3.360	8.212	0.0214	0.0488	0.9748
3181	0.036	0.096	0.169	4.693	5.873	4.073	0.0120	0.0317	0.9941
3330	0.040	0.204	0.345	8.526	2.888	1.645	0.0240	0.0693	0.9709
3331	0.119	0.228	0.339	2.861	2.751	2.582	0.0260	0.0721	0.9747
3332	0.203	0.257	0.365	1.799	2.762	3.479	0.0145	0.0538	0.9871
3340	0.126	0.183	0.322	2.549	2.253	2.259	0.0856	0.0553	0.9728
4000	0.068	0.122	0.172	2.530	4.302	2.162	0.0077	0.0331	0.9951
4001	0.081	0.121	0.168	2.066	4.911	2.006	0.0034	0.0206	0.9981
4010	0.020	0.058	0.122	6.041	10.434	3.334	0.0174	0.0439	0.9915
4011	0.017	0.063	0.130	7.483	4.471	1.712	0.0089	0.0315	0.9950
4020	0.033	0.081	0.144	4.410	4.037	1.963	0.0064	0.0303	0.9957
4021	0.038	0.087	0.145	3.828	4.070	2.082	0.0036	0.0227	0.9977
4050	0.029	0.085	0.152	5.295	5.468	1.883	0.0113	0.0375	0.9934
4051	0.052	0.106	0.163	3.157	4.774	3.058	0.0044	0.0250	0.9975
4052	0.045	0.094	0.153	3.376	4.680	1.838	0.0071	0.0319	0.9950
4061	0.060	0.106	0.153	2.547	5.709	2.169	0.0035	0.0222	0.9979
4130	0.021	0.099	0.191	8.959	11.147	1.831	0.0075	0.0328	0.9943
4132	0.042	0.071	0.124	2.975	10.029	3.806	0.0090	0.0358	0.9947
4142	0.065	0.116	0.173	2.644	5.181	2.447	0.0050	0.0267	0.9970
4152	0.056	0.104	0.162	2.877	6.310	1.832	0.0065	0.0305	0.9955
4520	0.121	0.165	0.255	2.106	4.803	4.505	0.0241	0.0468	0.9882
4521	0.121	0.165	0.255	2.106	4.803	4.505	0.0241	0.0468	0.9882
4522	0.121	0.165	0.255	2.106	5.243	7.036	0.0719	0.0809	0.9687
4523	0.121	0.165	0.255	2.106	5.243	7.036	0.0719	0.0809	0.9687
4650	0.072	0.231	0.376	5.201	2.195	2.007	0.0317	0.0371	0.9921
4651	0.084	0.227	0.389	4.646	1.677	2.013	0.0294	0.0358	0.9920
4660	0.065	0.217	0.355	5.488	0.501	1.475	0.0358	0.0394	0.9857
4661	0.072	0.229	0.363	5.022	0.790	1.739	0.0151	0.0256	0.9949

[a]SSE: sum of square errors; RMSE, root-mean-square error; and R^2, coefficient of determination.
[b]Soils with numbered IDs are from the UNSODA database.

Acknowledgments
This work was funded by the grant from F.R.S-FNRS of Belgium (Project PDR.T.1002.14 "Capillarity in granular materials"). The experimental data and more details about the theory development can be obtained by contacting Ji-Peng Wang via Ji-Peng.Wang@ulb.ac.be or Ji-Peng.Wang@outlook.com.

References

Alonso, E. E., J.-M. Pereira, J. Vaunat, and S. Olivella (2010), A microstructurally based effective stress for unsaturated soils, *Géotechnique*, *60*(12), 913–925, doi:10.1680/geot.8.P.002.

Arya, L. M., and J. F. Paris (1981), A physicoempirical model to predict the soil moisture characteristic from particle-size distribution and bulk density data, *Soil Sci. Soc. Am. J.*, *45*(6), 1023, doi:10.2136/sssaj1981.03615995004500060004x.

Arya, L. M., F. J. Leij, M. T. van Genuchten, and P. J. Shouse (1999), Scaling parameter to predict the soil water characteristic from particle-size distribution data, *Soil Sci. Soc. Am. J.*, *63*(3), 510, doi:10.2136/sssaj1999.03615995006300030013x.

Aubertin, M., M. Mbonimpa, B. Bussière, and R. P. Chapuis (2003), A model to predict the water retention curve from basic geotechnical properties, *Can. Geotech. J.*, *40*(6), 1104–1122, doi:10.1139/t03-054.

Baltodano-Goulding, R. (2006), Tensile strength, shear strength, and effective stress for unsaturated sand, PhD thesis, Univ. of Missouri Columbia, Columbia, Mo.

Bishop, A. W., and G. E. Blight (1963), Some aspects of effective stress in saturated and partly saturated soils, *Géotechnique*, *13*(3), 177–197, doi:10.1680/geot.1963.13.3.177.

Bouma, J. (1989), Using soil survey data for quantitative land evaluation, in *Advances in Soil Science*, pp. 177–213, Springer, New York.

Buckingham, E. (1914), On physically similar systems; illustrations of the use of dimensional equations, *Phys. Rev.*, *4*(4), 345–376, doi:10.1103/PhysRev.4.345.

Chiu, C. F., W. M. Yan, and K.-V. Yuen (2012), Estimation of water retention curve of granular soils from particle-size distribution—A Bayesian probabilistic approach, *Can. Geotech. J.*, *49*(9), 1024–1035, doi:10.1139/t2012-062.

Dane, J. H., and J. W. Hopmans (2002), Hanging water column, in *Methods of Soil Analysis: Part 4 Physical Methods*, edited by J. H. Dane and C. Topp, pp. 680–683, Soil Sci. Soc. of Am., Madison, Wis.

de Jong, R., and K. Loebel (1982), Empirical relations between soil components and water retention at 1/3 and 15 atmospheres, *Can. J. Soil Sci.*, *62*(2), 343–350, doi:10.4141/cjss82-038.

Feia, S., S. Ghabezloo, J. F. Bruchon, J. Sulem, J. Canou, and J. C. Dupla (2014), Experimental evaluation of the pore-access size distribution of sands, *Geotech. Test. J.*, *37*(4), 1–8, doi:10.1520/GTJ20130126.

Fredlund, D., H. Rahardjo, and J. Gan (1987), Non-linearity of strength envelope for unsaturated soils, in *Proceedings of the 6th International Conference on Expansive*, pp. 49–54, New Delhi, Boca Raton, Fla.

Fredlund, D. G., N. R. Morgenstern, and R. A. Widger (1978), The shear strength of unsaturated soils, *Can. Geotech. J.*, *15*(3), 313–321, doi:10.1139/t78-029.

Fredlund, D. G., A. Xing, M. D. Fredlund, and S. L. Barbour (1996), The relationship of the unsaturated soil shear to the soil-water characteristic curve, *Can. Geotech. J.*, *33*(3), 440–448, doi:10.1139/t96-065.

Fredlund, M. D., D. G. Fredlund, and G. W. Wilson (1997), Prediction of the soil-water characteristic curve from grain-size distribution and volume-mass properties, in *Proceedings of the 3rd Brazilian Symposium on Unsaturated Soils*, pp. 13–23, Rio de Janeiro, Brazil.

Fredlund, M. D., G. W. Wilson, and D. G. Fredlund (2002), Use of the grain-size distribution for estimation of the soil-water characteristic curve, *Can. Geotech. J.*, *39*(5), 1103–1117, doi:10.1139/t02-049.

Gallage, C. P. K., and T. Uchimura (2006), Effects of wetting and drying on the unsaturated shear strength of a silty sand under low suction, in *Unsaturated Soils 2006*, pp. 1247–1258, Am. Soc. of Civ. Eng., Reston, Va.

Gallage, C. P. K., and T. Uchimura (2010), Effects of dry density and grain size distribution on soil-water characteristic curves of sandy soils, *Soils Found.*, *50*(1), 161–172, doi:10.3208/sandf.50.161.

Ghanbarian-alavijeh, B., A. Liaghat, H. Guan-Hua, and M. Th. van Genuchten (2010), Estimation of the van Genuchten soil water retention properties from soil textural data, *Pedosphere*, *20*(4), 456–465, doi:10.1016/S1002-0160(10)60035-5.

Gupta, S. C., and W. E. Larson (1979), Estimating soil water retention characteristics from particle size distribution, organic matter percent, and bulk density, *Water Resour. Res.*, *15*(6), 1633–1635, doi:10.1029/WR015i006p01633.

Haverkamp, R., and J. Parlange (1986), Predicting the water-retention curve from particle-size distribution. 1. *Sandy soils without organic matter, Soil Sci.*, *142*(6), 325–339.

Hazen, A. (1892), *Physical Properties of Sands and Gravels With Reference to Their Use Infiltration*.

Hossain, M. A., and J.-H. Yin (2010), Shear strength and dilative characteristics of an unsaturated compacted completely decomposed granite soil, *Can. Geotech. J.*, *47*(10), 1112–1126, doi:10.1139/T10-015.

Hwang, S. I., and S. E. Powers (2003), Using particle-size distribution models to estimate soil hydraulic properties, *Soil Sci. Soc. Am. J.*, *67*(4), 1103, doi:10.2136/sssaj2003.1103.

Kenney, T. C., D. Lau, and G. I. Ofoegbu (1984), Permeability of compacted granular materials, *Can. Geotech. J.*, *21*(4), 726–729, doi:10.1139/t84-080.

Khalili, N., and M. H. Khabbaz (1998), A unique relationship for χ for the determination of the shear strength of unsaturated soils, *Géotechnique*, *48*(5), 681–687, doi:10.1680/geot.1998.48.5.681.

Kim, T.-H., and C. Hwang (2003), Modeling of tensile strength on moist granular earth material at low water content, *Eng. Geol.*, *69*(3–4), 233–244, doi:10.1016/S0013-7952(02)00284-3.

Kim, T.-H., and S. Sture (2008), Capillary-induced tensile strength in unsaturated sands, *Can. Geotech. J.*, *45*(5), 726–737, doi:10.1139/T08-017.

Konrad, J.-M., and M. Lebeau (2015), Capillary-based effective stress formulation for predicting shear strength of unsaturated soils, *Can. Geotech. J.*, *52*(12), 2067–2076, doi:10.1139/cgj-2014-0300.

Leij, F. J., W. J. Alves, M. T. van Genuchten, and J. R. Williams (1996), *The UNSODA Unsaturated Soil Hydraulic Database: User's Manual*, Natl. Risk Manage. Res. Lab., Off. of Res. and Dev., U.S. Environ. Prot. Agency, Washington, D. C.

Likos, W. J., A. Wayllace, J. Godt, and N. Lu (2010), Modified direct shear apparatus for unsaturated sands at low suction and stress, *Geotech. Test. J.*, *33*(4), 1–13, doi:10.1520/GTJ102927.

Lu, N., and W. J. Likos (2006), Suction stress characteristic curve for unsaturated soil, *J. Geotech. Geoenviron. Eng.*, *132*(2), 131–142, doi:10.1061/(ASCE)1090-0241(2006)132:2(131).

Lu, N., B. Wu, and C. P. Tan (2007), Tensile strength characteristics of unsaturated sands, *J. Geotech. Geoenviron. Eng.*, *133*(2), 144–154, doi:10.1061/(ASCE)1090-0241(2007)133:2(144).

Lu, N., T.-H. Kim, S. Sture, and W. J. Likos (2009), Tensile strength of unsaturated sand, *J. Eng. Mech.*, *135*(12), 1410–1419, doi:10.1061/(ASCE)EM.1943-7889.0000054.

Lu, N., J. W. Godt, and D. T. Wu (2010), A closed-form equation for effective stress in unsaturated soil, *Water Resour. Res.*, *46*, W05515, doi:10.1029/2009WR008646.

Matsushi, Y., and Y. Matsukura (2006), Cohesion of unsaturated residual soils as a function of volumetric water content, *Bull. Eng. Geol. Environ.*, *65*(4), 449–455, doi:10.1007/s10064-005-0035-9.

Mbonimpa, M., M. Aubertin, R. P. Chapuis, and B. Bussière (2002), Practical pedotransfer functions for estimating the saturated hydraulic conductivity, *Geotech. Geol. Eng.*, *20*(3), 235–259, doi:10.1023/A:1016046214724.

Minasny, B., A. B. McBratney, and K. L. Bristow (1999), Comparison of different approaches to the development of pedotransfer functions for water-retention curves, *Geoderma*, *93*(3), 225–253, doi:10.1016/S0016-7061(99)00061-0.

Oberg, A., and G. Sällfors (1997), Determination of shear strength parameters of unsaturated silts and sands based on the water retention curve, *Geotech. Test. J.*, *20*(1), 40, doi:10.1520/GTJ11419J.

Oh, S., and N. Lu (2014), Uniqueness of the suction stress characteristic curve under different confining stress conditions, *Vadose Zone J.*, *13*(5), 1–10, doi:10.2136/vzj2013.04.0077.

Oh, S., N. Lu, Y. K. Kim, S. J. Lee, and S. R. Lee (2012), Relationship between the soil-water characteristic curve and the suction stress characteristic curve: Experimental evidence from residual soils, *J. Geotech. Geoenviron. Eng.*, *138*(1), 47–57, doi:10.1061/(ASCE)GT.1943-5606.0000564.

Or, D., and M. Tuller (1999), Liquid retention and interfacial area in variably saturated porous media: Upscaling from single-pore to sample-scale model, *Water Resour. Res.*, *35*(12), 3591–3605, doi:10.1029/1999WR900262.

Patil, N. G., and S. K. Singh (2016), Pedotransfer functions for estimating soil hydraulic properties: A review, *Pedosphere*, *26*(4), 417–430, doi:10.1016/S1002-0160(15)60054-6.

Puckett, W. E., J. H. Dane, and B. F. Hajek (1985), Physical and mineralogical data to determine soil hydraulic properties, *Soil Sci. Soc. Am. J.*, *49*(4), 831, doi:10.2136/sssaj1985.03615995004900040008x.

Rawles, W., and D. Brakensiek (1982), Estimating soil water retention from soil properties, *J. Irrig. Drain.*, *108*(2), 166–171.

Saxton, K. E., W. J. Rawls, J. S. Romberger, and R. I. Papendick (1986), Estimating generalized soil-water characteristics from texture, *Soil Sci. Soc. Am. J.*, *50*(4), 1031, doi:10.2136/sssaj1986.03615995005000040039x.

Schaap, M. G., and W. Bouten (1996), Modeling water retention curves of sandy soils using neural networks, *Water Resour. Res.*, *32*(10), 3033–3040, doi:10.1029/96WR02278.

Schaap, M. G., and F. J. Leij (1998), Using neural networks to predict soil water retention and soil hydraulic conductivity, *Soil Tillage Res.*, *47*(1), 37–42, doi:10.1016/S0167-1987(98)00070-1.

Schaap, M. G., F. J. Leij, and M. T. van Genuchten (2001), ROSETTA: A computer program for estimating soil hydraulic parameters with hierarchical pedotransfer functions, *J. Hydrol.*, *251*(3–4), 163–176, doi:10.1016/S0022-1694(01)00466-8.

Scheel, M., R. Seemann, M. Brinkmann, M. Di Michiel, A. Sheppard, B. Breidenbach, and S. Herminghaus (2008), Morphological clues to wet granular pile stability, *Nat. Mater.*, *7*(3), 189–193, doi:10.1038/nmat2117.

Scheinost, A. C., W. Sinowski, and K. Auerswald (1997), Regionalization of soil water retention curves in a highly variable soilscape, I. Developing a new pedotransfer function, *Geoderma*, *78*(3–4), 129–143, doi:10.1016/S0016-7061(97)00046-3.

Schubert, H. (1984), Capillary forces—Modeling and application in particulate technology, *Powder Technol.*, *37*(1), 105–116, doi:10.1016/0032-5910(84)80010-8.

Schubert, H., W. Herrmann, and H. Rumpf (1975), Deformation behaviour of agglomerates under tensile stress, *Powder Technol.*, *11*(2), 121–131, doi:10.1016/0032-5910(75)80037-4.

Tekinsoy, M. A., C. Kayadelen, M. S. Keskin, and M. Söylemez (2004), An equation for predicting shear strength envelope with respect to matric suction, *Comput. Geotech.*, *31*(7), 589–593, doi:10.1016/j.compgeo.2004.08.001.

Terzaghi, K., R. Peck, and G. Mesri (1996), *Soil Mechanics in Engineering Practice*, John Wiley, New York.

Tuller, M., D. Or, and L. M. Dudley (1999), Adsorption and capillary condensation in porous media: Liquid retention and interfacial configurations in angular pores, *Water Resour. Res.*, *35*(7), 1949–1964, doi:10.1029/1999WR900098.

Turner, G. A., M. Balasubramanian, and L. Otten (1976), The tensile strength of moist limestone powder. Measurements by different apparatuses, *Powder Technol.*, *15*(1), 97–105, doi:10.1016/0032-5910(76)80034-4.

Tyler, S. W., and S. W. Wheatcraft (1989), Application of fractal mathematics to soil water retention estimation, *Soil Sci. Soc. Am. J.*, *53*(4), 987–996, doi:10.2136/sssaj1989.03615995005300040001x.

van Genuchten, M. T. (1980), A closed-form equation for predicting the hydraulic conductivity of unsaturated soils, *Soil Sci. Soc. Am. J.*, *44*(5), 892–898.

Vanapalli, S. K., and D. G. Fredlund (2000), Comparison of different procedures to predict unsaturated soil shear strength, in *Advances in Unsaturated Geotechnics*, pp. 195–209, Am. Soc. of Civ. Eng., Reston, Va.

Vanapalli, S. K., D. G. Fredlund, D. E. Pufahl, and A. W. Clifton (1996), Model for the prediction of shear strength with respect to soil suction, *Can. Geotech. J.*, *33*(3), 379–392, doi:10.1139/t96-060.

Vereecken, H., J. Maes, J. Feyen, and P. Darius (1989), Estimating the soil moisture retention characteristic from texture, bulk density, and carbon content, *Soil Sci.*, *148*(6), 389–403, doi:10.1097/00010694-198912000-00001.

Vereecken, H., M. Weynants, M. Javaux, Y. Pachepsky, M. G. Schaap, and M. T. van Genuchten (2010), Using pedotransfer functions to estimate the van Genuchten–Mualem soil hydraulic properties: A review, *Vadose Zone J.*, *9*(4), 795, doi:10.2136/vzj2010.0045.

Vienken, T., and P. Dietrich (2011), Field evaluation of methods for determining hydraulic conductivity from grain size data, *J. Hydrol.*, *400*(1–2), 58–71, doi:10.1016/j.jhydrol.2011.01.022.

Wang, J.-P., E. Gallo, B. François, F. Gabrieli, and P. Lambert (2017), Capillary force and rupture of funicular liquid bridges between three spherical bodies, *Powder Technol.*, *305*, 89–98, doi:10.1016/j.powtec.2016.09.060.

Wösten, J. H. M., and M. T. van Genuchten (1988), Using texture and other soil properties to predict the unsaturated soil hydraulic functions, *Soil Sci. Soc. Am. J.*, *52*(6), 1762, doi:10.2136/sssaj1988.03615995005200060045x.

Yang, H., H. Rahardjo, E.-C. Leong, and D. G. Fredlund (2004), Factors affecting drying and wetting soil-water characteristic curves of sandy soils, *Can. Geotech. J.*, *41*(5), 908–920, doi:10.1139/t04-042.

Zhou, A., R. Huang, and D. Sheng (2016), Capillary water retention curve and shear strength of unsaturated soils, *Can. Geotech. J.*, *53*(6), 974–987, doi:10.1139/cgj-2015-0322.